

Simulated climate change effects on ice and snow covers on lakes in a temperate region

Heinz G. Stefan^a, Xing Fang^b

^a University of Minnesota, Department of Civil Engineering, Minneapolis, MN 55414, USA

^b Lamar University, Department of Civil Engineering, Beaumont, TX 77710, USA

Received 15 July 1996; accepted 7 October 1996

Abstract

A simulation model for ice and snow covers is applied to dimictic and polymictic lakes of the temperate zone to project the effects of possible climate warming on ice and snow covers. The winter cover model is associated with a deterministic, one-dimensional water temperature model. The lake parameters required as model input are surface area (A_S), maximum depth (H_{\max}), summer and Secchi depth as a measure of radiation attenuation and trophic state. The model is driven by daily weather data. The model has been validated with extensive data. Standard errors between simulated and measured values are 0.12 m for ice thicknesses, 0.07 m for snow covers and less than 6 days for ice formation dates. The model is applied to simulate effects of projected climate change on winter ice and snow covers on different types of lakes in Minnesota. Lake depth and latitude are shown to have the strongest influence on freeze-over dates. Lake morphometry causes variations of up to 6 days in the mean value of ice-in dates. The trophic state and shape of a lake have little effect on ice-out date, but latitude is important.

The projected climate change due to a doubling of atmospheric carbon dioxide ($2 \times \text{CO}_2$) is obtained from the output of the Canadian Climate Center Global Circulation Model (CCC GCM) and the Goddard Institute of Space Studies at Columbia University (GISS GCM). The $2 \times \text{CO}_2$ climate delays the ice formation by as much as 20 days, reduces maximum ice and snow thicknesses by 50%, and shortens the ice cover period by up to 60 days. These changes would eliminate fish winterkill in most shallow lakes, but would endanger snowmobiles and ice fishermen. To illustrate the effect of projected climate change on winter ice/snow cover characteristics, separate graphs are presented for values simulated with inputs of past climate conditions (1961–79) and with a projected $2 \times \text{CO}_2$ climate scenario. Independent variables used on these plots are a lake geometry ratio $A_S^{0.25}/H_{\max}$ and Secchi depth. The lake geometry ratio measures the susceptibility of a lake to stratification.

Keywords: Simulation; Climate change effects; Ice cover; Snow cover; Temperate region

1. Introduction

In cold regions, transfer processes which normally occur through the open-water surface of a lake are substantially altered by ice and snow covers. Ice formation on small freshwater lakes generally occurs on a calm, cold night. Rising winds and daytime

heating may subsequently break up this cover until calm and cold conditions occur again and the ice cover forms a second time (Ashton, 1986). The ice formation date is usually associated with the coldest water temperature in a lake (Stefan and Fang, 1995). An ice cover on a lake stops oxygen exchange (reaeration) between the atmosphere and the water.

As a consequence dissolved oxygen concentration, which is essential to many aquatic organisms in a lake, diminishes after an ice cover has formed due to sedimentary and water column oxygen demand. With an additional snow cover on a lake, most light attenuates within the snow, and therefore photosynthetic oxygen production by plants reaches zero. Fish winterkill can occur in shallow lakes near the end of the ice cover period (early spring) when dissolved oxygen concentrations drop below 2 mg/l. This is but one example of how an ice/snow cover on a lake influences water quality and ecology in a lake.

This paper summarizes results obtained with a model that simulates the formation and the character-

istics of ice/snow covers on lakes and the associated daily water temperature profiles in lakes using daily weather data as input. The model includes sediment heat exchange in all layers of a lake. This is most important for the simulation of ice covered lakes because heat released from the sediment during the winter warms the lake water under the ice. Coefficients in the model are derived from extensive data from Minnesota lakes (Table 1). The model is thus a “regional” model which is applied without further calibration.

Because the model is driven by daily weather parameters as input, it can be used to study the effects of climate change on lake ice/snow covers.

Table 1
Parameters and coefficient values used in the model

Parameters and symbols		Units	Range and references	Selected value
<i>Open water season</i>				
Radiation absorption for water	β_w	—	0.4 ^a	0.4
Sediment specific heat	c_{psed}	kcal kg ⁻¹ °C ⁻¹	0.2–0.3 ^b	0.28
Sediment thermal conductivity	k_{sed}	kcal day ⁻¹ °C ⁻¹ m ⁻¹	8.64–51.8 ^b	19.25
Radiation attenuation by Chl-a	μ_{ch}	m ² g ⁻¹ Chl-a	0.2–31.5 ^c	20.0
Radiation attenuation by water	μ_w	m ⁻¹	0.33–1.03 ^d	0.51
Sediment density	ρ_{sed}	kg m ⁻³	1650–2300 ^b	1970
Wind sheltering	W_{str}	—	0.01–1.0 ^e	varies
<i>Winter ice cover</i>				
Surface reflectivity for ice	α_i	—	0.55 ^h	0.55
Surface reflectivity for snow	α_{sw}	—	0.4–0.95 ^l	0.80
Radiation absorption for ice	β_i	—	0.17–0.32 ^f	0.17
Radiation absorption for snow	β_{sw}	—	0.17–0.34 ^g	0.34
Snow compaction	c_{sw}	—	0.125–0.5 ^l	0.4
Ice thermal conductivity	k_i	kcal day ⁻¹ °C ⁻¹ m ⁻¹	45.8 ^b	53.6
Snow thermal conductivity	k_{sw}	kcal day ⁻¹ °C ⁻¹ m ⁻¹	2.16 ^b	5.57
Ice density	ρ_i	kg m ⁻³	920 ^b	920.0
Snow density	ρ_{sw}	kg m ⁻³	100–400 ^l	300.0
Radiation attenuation by ice	μ_i	m ⁻¹	1.6–7.0 ^j	1.6
Radiation attenuation by snow	μ_{sw}	m ⁻¹	20–40 ⁱ	40.0
Ice latent heat of fusion	λ_i	kcal kg ⁻¹	80 ^k	80.0
Snow latent heat of fusion	λ_{sw}	kcal kg ⁻¹	80 ^k	80.0

^a Dake and Harleman, 1969.

^b Carslaw and Jaeger, 1959.

^c Bannister, 1974.

^d Megard et al., 1979.

^e Riley and Stefan, 1987.

^f Wake and Rumer, 1979.

^g Scott, 1964.

^h Bolsenga, 1977.

ⁱ Greene, 1981.

^j Pivovarov, 1972.

^k Ashton, 1986.

^l Lock, 1934.

To project potential effects of climate change on lake water quality (e.g. water temperature, dissolved oxygen, nutrients) and ecology of lakes in cold regions, ice formation and ice/snow covers on lakes have to be simulated first. To do this, projected changes in climate conditions were obtained from the output of the Canadian Climate Center Global Circulation Model (CCC GCM) and the Goddard Institute of Space Studies at Columbia University (GISS GCM) for a doubling of atmospheric CO₂. The monthly differences between the present (1 × CO₂) and projected (2 × CO₂) climate scenarios were applied to measured past climate conditions from 1961 to 1979. Results on winter covers of lakes in Minnesota are given herein for both past and 2 × CO₂ climate scenarios.

2. Model development

2.1. Ice-cover and water temperature model

The numerical simulation model for water temperature profiles in cold climate lakes solves the one-dimensional, unsteady heat transfer equation

$$\frac{\partial T_w}{\partial t} = \frac{1}{A} \frac{\partial}{\partial z} \left[K_z A \frac{\partial T_w}{\partial z} \right] + \frac{\phi_w}{\rho c_p} \quad (1)$$

where T_w (°C) is the water temperature, t (day) is the time, A (m²) is the horizontal area as a function of depth z (m), K_z (m² day⁻¹) is the vertical turbulent

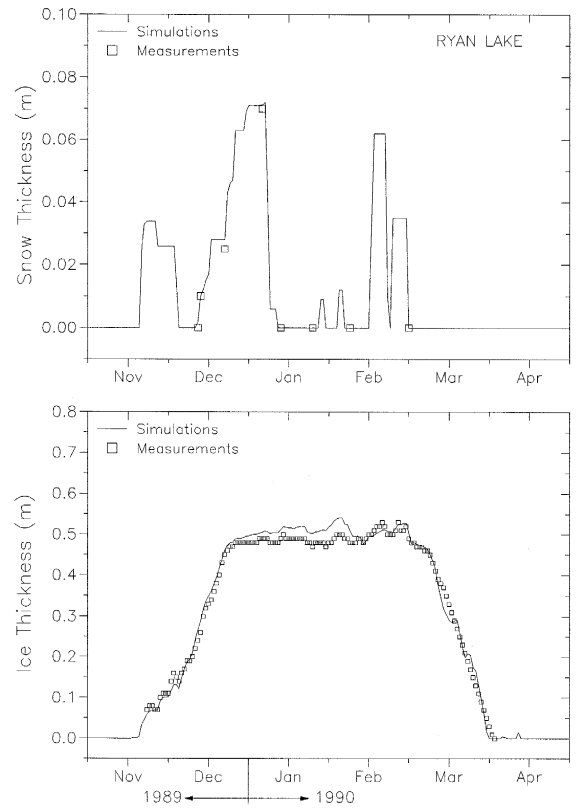


Fig. 2. Simulated and measured ice thicknesses and snow depths on Ryan Lake, Minnesota.

heat diffusion coefficient, ρc_p (J m⁻³ °C⁻¹) represents heat capacity per unit volume and is the density of water (ρ) times heat capacity of water (c_p), and

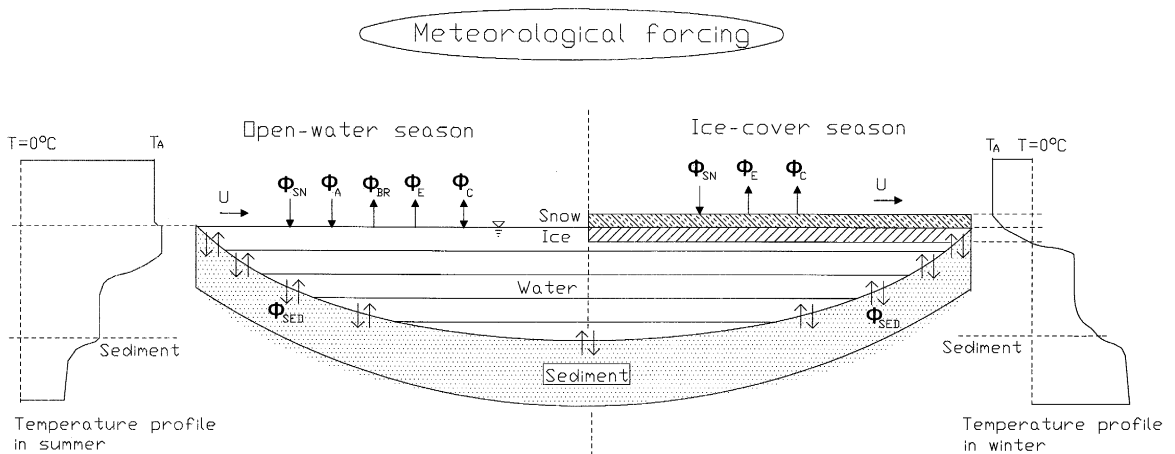


Fig. 1. Schematic diagram of a stratified lake showing heat transfer components and temperature profiles in summer and winter.

ϕ_w ($J m^{-3} day^{-1}$) is the heat source or sink strength per unit volume. Solar radiation absorption in the water column makes a contribution to the heat source term. Heat exchange between the lake and the atmosphere is treated as a source/sink term for the topmost water layer in a lake during the open water season (Fig. 1). The determination of source and sink terms and the computational scheme have been discussed, e.g., by Edinger et al. (1968), Ford and Stefan (1980), Harleman (1982), and Hondzo and Stefan (1993a), among others. Eq. (1) is solved numerically using an implicit finite-difference scheme and a Gaussian elimination method. Timesteps of one day and layer thicknesses of one meter were used.

The snow and ice thickness submodels were originally developed by Gu and Stefan (1990), but have been used with some modifications. A new algorithm replacing the previous empirical and lake size depen-

dent criteria to predict the date of ice formation has been developed and incorporated in the new model (Fang et al., 1996). The new algorithm uses a full heat budget equation to estimate surface cooling, quantifies the effect of forced convective (wind) mixing and includes the latent heat removed by ice formation. The algorithm has a fine spatial resolution near the water surface where temperature gradients before freeze-over are the greatest.

The water temperature simulation model has also been expanded significantly from its previous version (Hondzo and Stefan, 1993a) by including the heat exchange ϕ_{sed} between each water layer and its adjoining sediments (Fig. 1). Although a boundary condition, the sediment/water heat flux is treated as a contribution to the source/sink term for each water layer from the water surface to the lake bottom (Fang and Stefan, 1996a). On a seasonal timescale heat is transferred from water to lake sediments

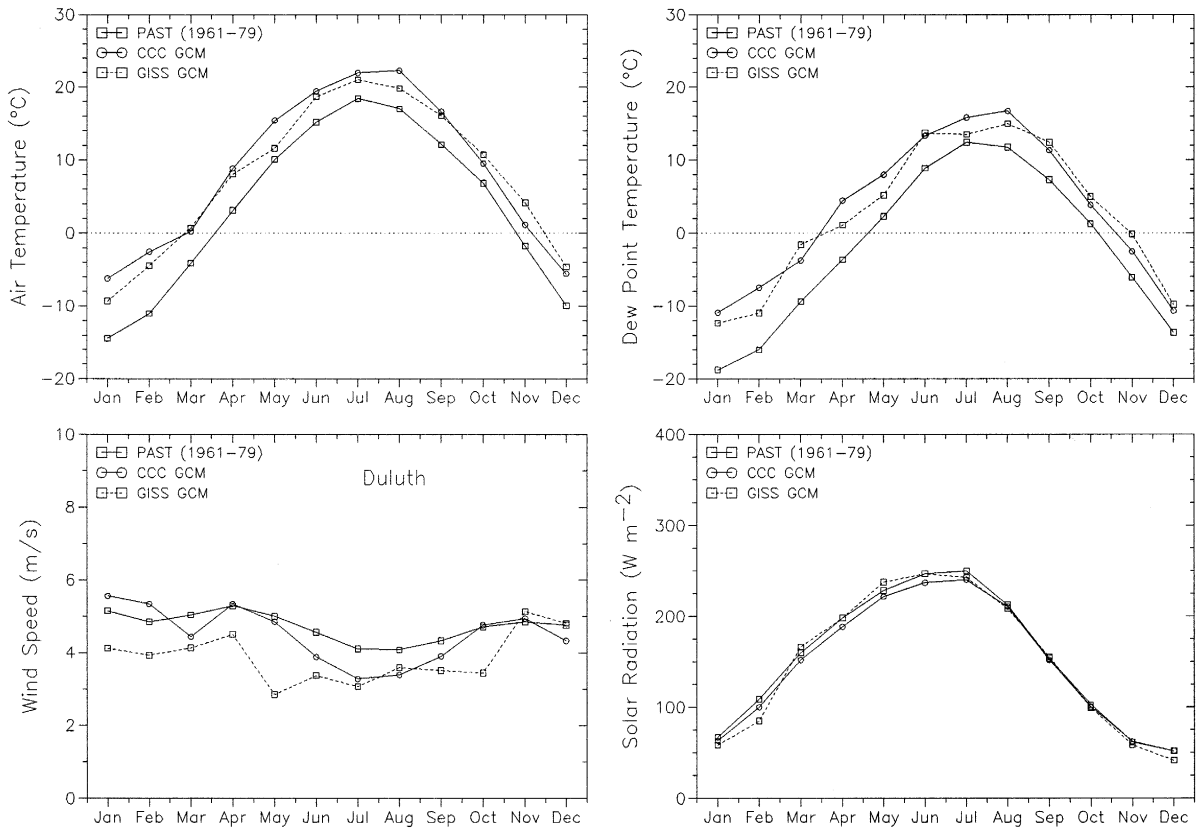


Fig. 3. Past (1961–1979) and projected $2 \times CO_2$ climate scenarios (CCC GCM and GISS GCM). Monthly averages of air temperature ($^{\circ}C$), dew point temperature ($^{\circ}C$), wind speed ($m s^{-1}$) and solar radiation ($W m^{-2}$) at Duluth Airport, Minnesota.

during the summer and released from lake sediments into the water during the winter. However the direction of the heat flux reverses frequently on shorter, e.g. daily timescales (Fang and Stefan, 1996b). Heat can transfer into or out of the lake sediment during both the open water season and the winter ice cover period. Therefore the lake sediments not only provide seasonal heat storage, but also add significant thermal inertia to the lake. Sediment heat fluxes are most important in winter, particularly for shallow lakes. Other features of the winter water temperature model include a new expression for vertical turbulent diffusion coefficients during the ice cover period

(Ellis and Stefan, 1997) and adaptation of the computational scheme proposed by Pivovarov (1972).

During the ice cover period, the model simulates ice thicknesses and sediment temperature profiles (heat conduction equation) first, then determines the heat source/sink term ϕ_w in Eq. (1), and finally solves the heat transfer Eq. (1) to obtain water temperature profiles below the ice. The model uses a stacked layer system, the layers consisting of lake sediments, water, ice cover and snow cover (Fig. 1). At the air/snow interface (or air/ice interface if snow is absent), the net heat flux from the atmosphere into or out of the snow/ice cover is calcu-

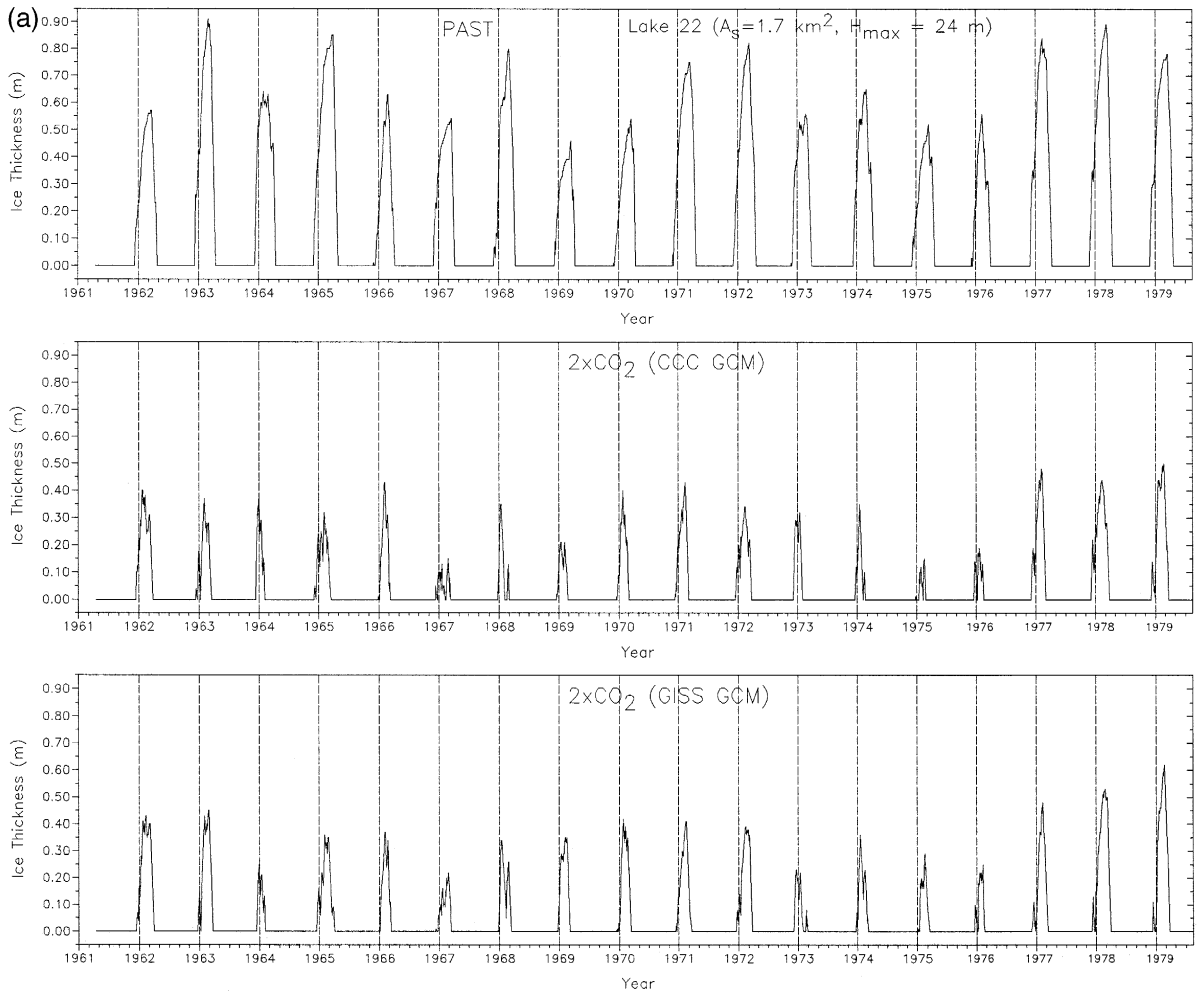


Fig. 4. (a) Simulated ice thicknesses on a medium surface area, deep lake (Lake 22) under three climate scenarios. (b) Simulated snow depths on a medium surface area, deep lake (Lake 22) under three climate scenarios.

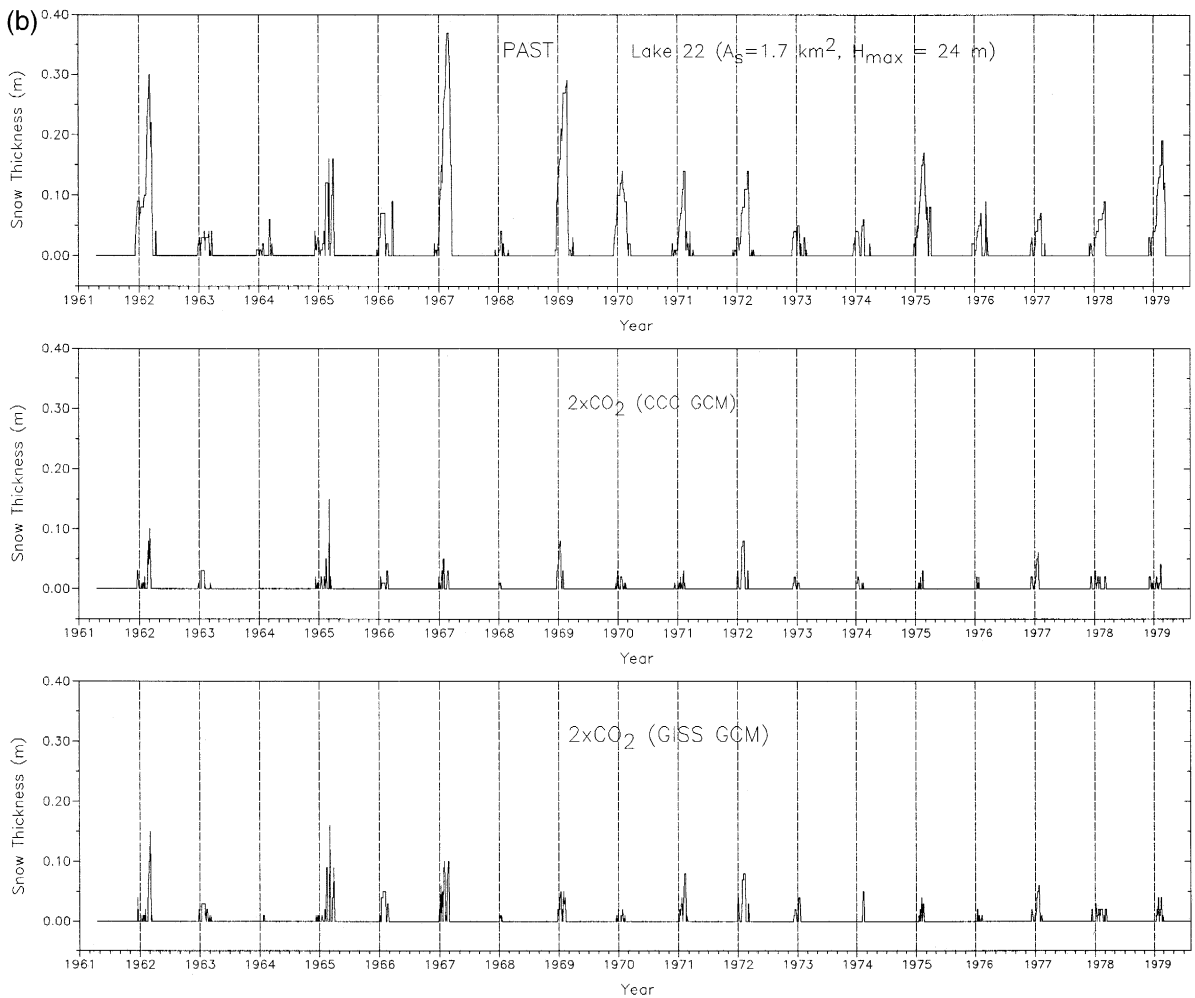


Fig. 4. (continued).

lated. Contributions are made by solar radiation (ϕ_{SN}), evaporation (ϕ_E) and convection (ϕ_C). The latter two are functions of the wind speed U . Atmospheric radiation ϕ_A and backradiation ϕ_{BR} are assumed to balance in winter (Gu and Stefan, 1990). Snow thickness is determined from snow accumulation, followed by compaction and melting of snow by surface heat input (convection, rainfall, solar radiation) and melting within the snow layer due to internal absorption of short wave radiation. In the model ice growth occurs only at the ice/water interface, but ice can decay at the snow/ice interface, the ice/water interface, and within the ice layer. The

complete set of equations used has been summarized by Fang and Stefan (1994).

2.2. Model validation

Ice formation dates are directly related to the rate of surface cooling and the amount of heat stored in a lake in summer. The water temperature model was therefore calibrated against measured temperature profiles in nine Minnesota lakes. Measurements were available for selected years from 1980 to 1993, a total of 48 “lake years” during the open water season (over 5,000 data pairs). The average standard

error between simulated and measured water temperatures was 1.4°C with a range from 0.92 to 1.69°C.

Measured ice thicknesses, snow depths and water temperatures under the ice cover for Ryan Lake, Minnesota (from 1989 to 1995), Thrush Lake, Minnesota (from 1986 to 1991) and Little Rock Lake, Wisconsin (from 1983 to 1991) were used for model validation (Fang and Stefan, 1996a). Standard errors between simulated and measured values were 0.07 m for snow depths and 0.12 m for ice thicknesses for long-term simulations (128 data pairs of ice/snow measurements over 8 years) in Thrush Lake and Little Rock Lake. Average standard error between simulated and measured water temperatures during the ice cover season was 0.5°C for these two lakes. Predicted freeze-over dates were compared with observations in nine Minnesota lakes for multiple (1 to 36) years (Fang et al., 1996). The difference between the simulated and observed ice formation dates was less than 6 days for all lakes studied. As an example, simulated ice and snow thicknesses in Ryan Lake, Minnesota, are shown in Fig. 2. The standard error between simulated and measured ice thicknesses in Ryan Lake was 0.02 m as shown.

3. Model inputs

3.1. Lake types

Lakes were classified into 27 types (Stefan et al., 1992) based on surface area (A_s), maximum lake depth (H_{\max}) and trophic state. Representative values for surface area were selected to be 0.2, 1.7, and 10 km² for small, medium and large lakes, respectively. Maximum depths selected for shallow, medium and deep lakes were 4, 13 and 24 m, respectively. Secchi depth was used to represent trophic state of a lake. Secchi depths of 1.2, 2.5, 4.5 m for eutrophic, mesotrophic and oligotrophic lakes were chosen, respectively. Also, all Minnesota lakes were divided into two regions, southern and northern Minnesota, because there is a significant “break” in geological, topographic, hydrological, climatological and ecological parameters across the mid-section of the state (Baker et al., 1985; Heiskary et al., 1987).

The lake morphometry (hypographic curve or depth–area curve) is one of the model input parameters. Representative area–depth relationships for dif-

Table 2
Parameters used to define long-term winter ice-cover characteristics

Parameter	Description	Formulation/definition
Earliest ice-in date (T_{ei})	First day with ice cover in fall, but ice may melt out	–
Latest ice-in date	Last day with open water in fall; followed by ice growth and winter ice cover	–
Earliest ice-out date	First day without ice cover in spring, but ice cover may form again	–
Latest ice-out date (T_{io})	Last day with ice cover in spring; followed by open water season	–
Duration of ice cover	Total number of days with lake ice cover (D_{ice})	–
Total period of ice cover	Days between earliest ice-in and latest ice-out dates	$T_{io} - T_{ei}$
Continuous ice cover ratio	Duration of ice cover divided by total period of ice cover	$\frac{D_{ice}}{T_{io} - T_{ei}}$
Maximum ice thickness (m)	Maximum ice thickness over winter ice cover period	$\text{Max}[\delta_t, t = 1, 365]$
Average snow depth (m)	Cumulative snow depth on ice divided by duration of ice cover	$\frac{\sum \delta_{\text{snow}}}{D_{ice}}$
Continuous snow cover ratio	Number of days with snow cover divided by duration of ice cover	$\frac{\sum_{T_{io}}^{T_{ei}} \delta_{\text{snow}} > 0}{D_{ice}}$

ferent lake classes in Minnesota were specified by an equation of the form

$$\frac{A(z)}{A_s} = a \exp\left(b \frac{z}{H_{\max}}\right) + c \quad (3)$$

where $A(z)$ is the horizontal area at depth z below water surface. Regression coefficients (a, b, c) were obtained from data for 122 Minnesota lakes (Hondzo and Stefan, 1993b).

3.2. Past and $2 \times CO_2$ climate scenarios

Weather data are model inputs and consist of daily air temperature, dew point temperature, wind speed, solar radiation, total cloud cover, and precipitation (both rainfall and snowfall). Past climate con-

ditions were modelled with weather data from 1961 to 1979, obtained from the National Climatic Data Center (CD SAMSON). During this period the climate was relatively stable, i.e. no trends appeared in the data, although variability existed, of course, from year to year. Meteorological data collected at the Minneapolis/St. Paul Airport and the Duluth Airport were used for northern and southern Minnesota, respectively.

The outputs of the Goddard Institute of Space Studies Global Circulation Model (GISS GCM) and of the Canadian Climate Center Second-Generation General Circulation Model (CCC GCM) (McFarlane et al., 1992; Boer et al., 1992) were used to specify the increments in monthly climatic parameter values representative of a doubling of atmospheric CO_2 .

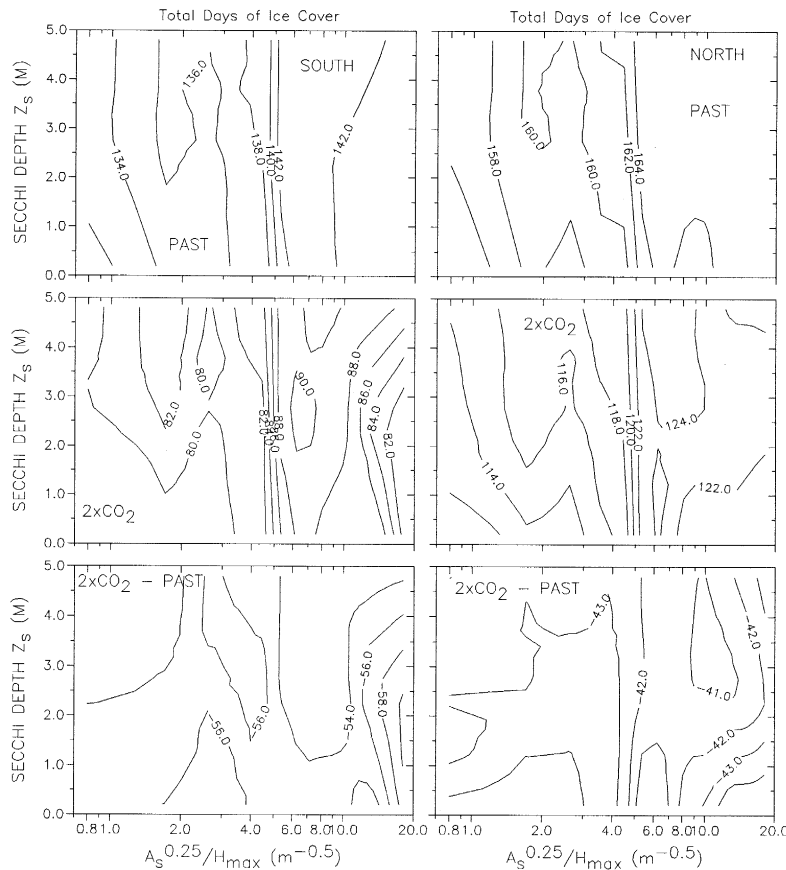


Fig. 5. Simulated total days of ice cover in southern (left) and northern (right) Minnesota lakes plotted as isopleths against two lake parameters. Past conditions (top), projected $2 \times CO_2$ CCC GCM climate scenario (middle), and differences between $2 \times CO_2$ and past climate conditions (bottom).

The second generation model (CCC GCM) includes higher spatial resolution $3.75^\circ \times 3.75^\circ$ than previous models and full diurnal and annual cycles. The global annual increases in surface air temperature simulated by the GISS and the CCC models are 4.2 and 3.5°C, respectively.

Monthly climate parameter increments obtained from GCMs were applied to the past climate conditions (1961 to 1979) to generate the future $2 \times \text{CO}_2$ climate scenario. The GCM outputs were taken from the grid points nearest Minneapolis and Duluth. No interpolation with other grid points was performed in agreement with EPA recommendations for climate effect studies. For the GISS model, these grid points were located outside Minnesota. For the CCC model, the grid point closest to both Minneapolis and Du-

luth is located centrally within Minnesota. The same mean monthly adjustments for both southern and northern Minnesota were therefore used for the CCC. The average increases of air temperatures during the cold season (November to March) and the warm season (April to October) were 6.4 and 4.3°C, respectively. Fig. 3 shows 19-year averages of monthly weather parameters for both past and $2 \times \text{CO}_2$ climate scenarios for the southern part as an example. Those derived from the GISS model were previously given by Hondzo and Stefan (1993b).

The accuracy of the GCM's is not without debate but difficult to quantify, especially for $2 \times \text{CO}_2$ conditions. At present, the GISS and the CCC are considered to be among the more reliable GCM's. The outputs of several GCM's have been compared

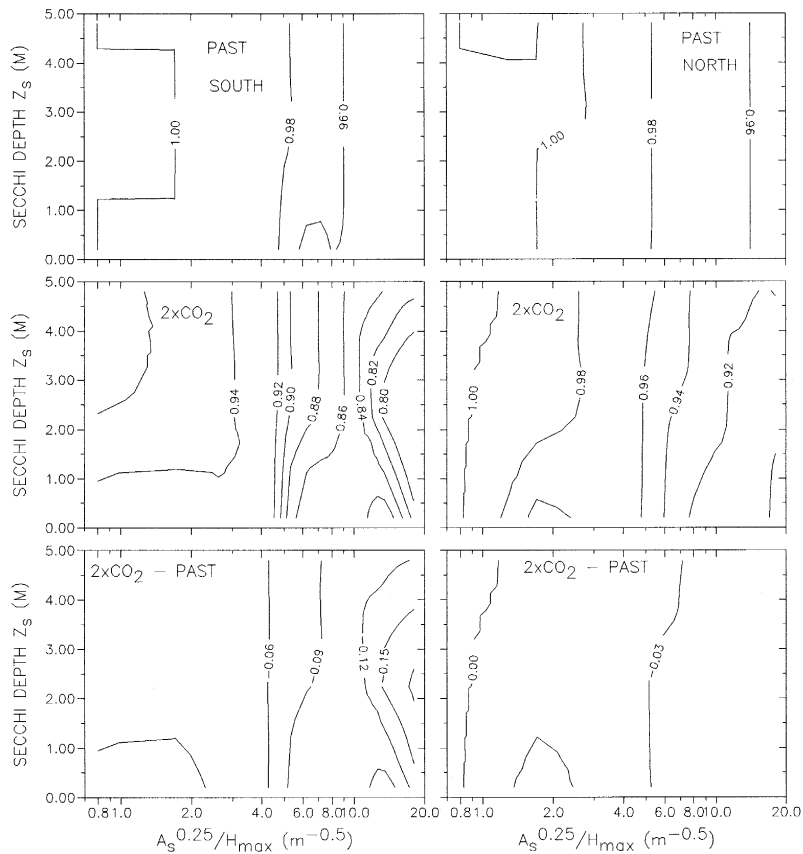


Fig. 6. Simulated continuous ice cover ratio in southern (left) and northern (right) Minnesota lakes plotted against two lake parameters. Past conditions (top), projected $2 \times \text{CO}_2$ CCC GCM climate scenario (middle), and differences between $2 \times \text{CO}_2$ and past climate conditions (bottom).

at various times, and a widely shared assessment is that of all the climate parameters simulated by GCM's, the most reliable is air temperature. This parameter has a very direct and immediate influence on ice and snow covers. Moisture related parameters, e.g. cloud cover, are less reliably simulated. Any uncertainty in the GCM output is, of course, carried over into the heat budget equations which affect ice and snow covers. The uncertainty/accuracy of the ice/snow cover model for past ($1 \times \text{CO}_2$) climate has been assessed; for the projected ($2 \times \text{CO}_2$) climate scenario this is, however, much more difficult to do.

4. Simulated winter cover characteristics

Time series plots of simulated ice thicknesses (Fig. 4a) and snow depths (Fig. 4b) for the 19-year (1961–79) simulation period are shown for the lake class 22 as an example. The variability from year to year is pronounced. A 19-year average value of maximum ice thickness is on the order of 0.59 m in the south and 0.67 m in the north for all lakes under past climate conditions (Stefan and Fang, 1995). Variations among lakes of different size, depth, and trophic state are no more than 10% or 0.05 m. The largest daily ice thickness in the entire simulation period of 19 years is about 50% larger than the 19-year average. Results obtained for $2 \times \text{CO}_2$ climate scenarios (CCC and GISS GCM) are plotted in Fig. 4a and b for comparison with those for past climate conditions. Maximum ice thicknesses are projected to become about half the present values, i.e. on the average 0.25 m and 0.40 m in the south and north (Stefan and Fang, 1995), respectively. This will occur because under the $2 \times \text{CO}_2$ climate scenarios the period of ice growth will be shortened. Nineteen-year averages of maximum cumulative (compacted) snow depths are only 10 cm and 20 cm in the south and north under past climate, respectively. The cumulative snow depths are projected to be reduced by even more than half if the $2 \times \text{CO}_2$ climate scenario becomes reality.

Ten parameters defined in Table 2 were selected to quantify the characteristics of ice and snow covers on lakes. The selected characteristics have all ecological significance, e.g. for water temperature and dis-

solved oxygen, consequently the survival and growth of fishes. Since the main objective of the investigation was to identify trends/changes in lake characteristics in response to climate change, and not extreme values which may occur over a 19-year (1961–1979) period, the 19 values of simulated parameters were averaged.

Herein examples of ice cover characteristics were plotted against lake surface area, maximum lake depth, and Secchi depth. The surface area, A_s , and maximum depth, H_{\max} , were combined in a lake geometry ratio ($A_s^{0.25}/H_{\max}$) which was previously shown (Gorham and Boyce, 1989; Stefan et al., 1993) to be a good relative measure of a lake's susceptibility to stratify; Secchi depth z_s was retained as a measure of lake transparency and trophic state. To show the effect of latitude, the results for the southern and northern half of Minnesota are presented separately. Results on the left side of Figs. 5–8 are for climate recorded at $44^\circ 53' \text{N}$ latitude and labeled "south", those on the right are for climate at $46^\circ 50' \text{N}$, a 2° latitudinal difference, and labeled "north". The values projected for a doubling of atmospheric CO_2 are given in the row labeled " $2 \times \text{CO}_2$ ". The differences between values simulated with projected $2 \times \text{CO}_2$ climate scenario and historical (1961–1979) weather data as input are shown in the bottom row and labelled " $2 \times \text{CO}_2$ — PAST".

The *total duration of ice cover* (Fig. 5) is the total number of days when an ice cover is present on a lake. Total duration of ice cover is presently about 140 days in southern Minnesota, and about 160 days in northern Minnesota. It will be shortened by about 55 days and 40 days, respectively, under a $2 \times \text{CO}_2$ climate scenario. Lake geometry (area and depth) is of some influence; lake trophic state has virtually no influence on the length of the ice cover period.

The *continuous ice cover ratio* (Fig. 6) measures whether an ice cover is continuous or discontinuous. It is calculated as the number of days with ice cover divided by the total period of ice cover defined as the period from first freeze-over to last ice-out. A value of 1.0 indicates a continuous ice cover. Ice covers are more continuous in northern than in southern Minnesota (Fig. 6). After climate warming, they are projected to be less continuous in both the south and the north. A discontinuous ice-cover is one that melts and then forms again at least once in a

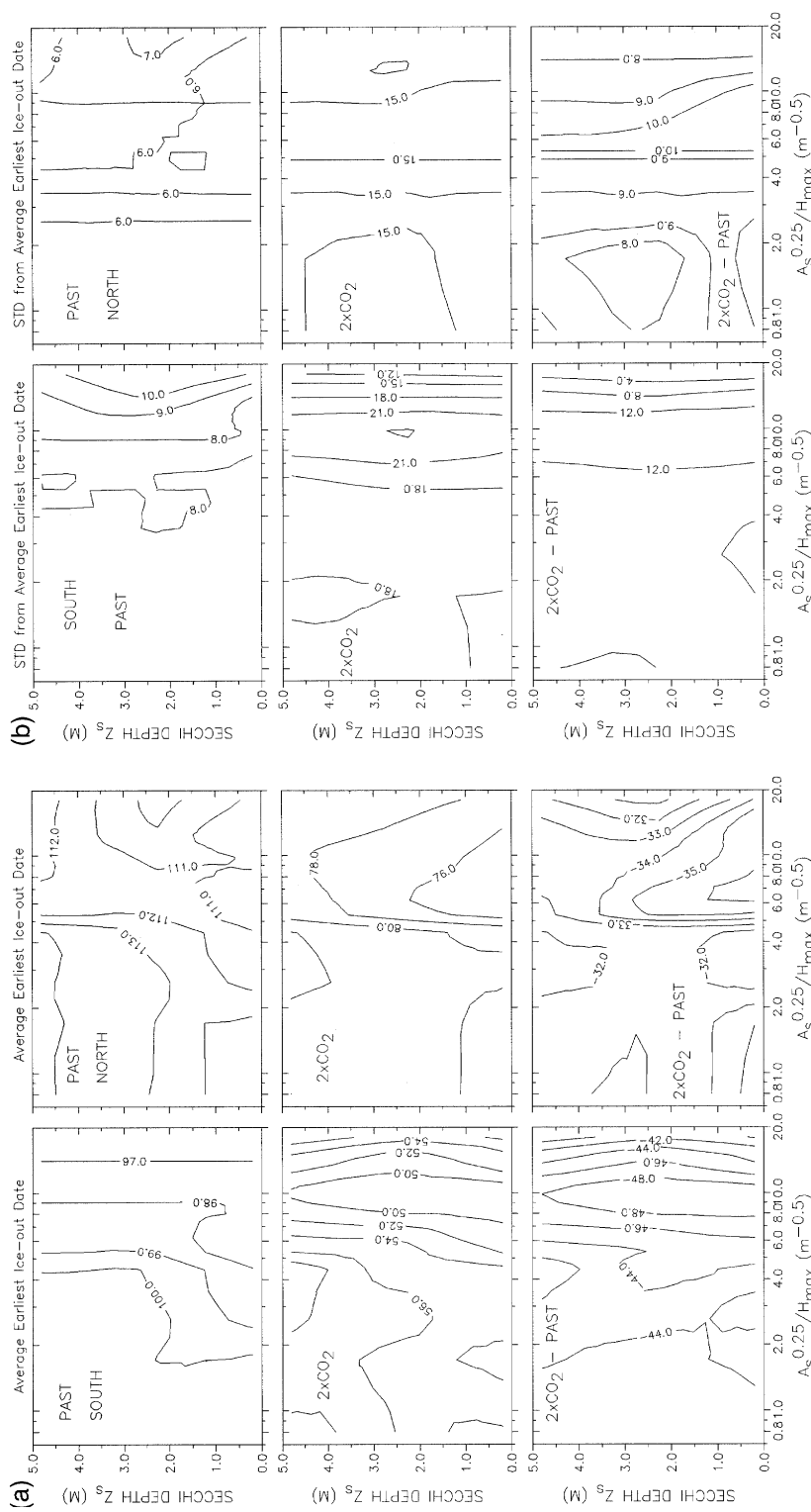


Fig. 8. Simulated average ice-out dates (a) and standard deviation (STD) from simulated average earliest ice-out dates (b) in southern (left) and northern (right) Minnesota lakes plotted as isopleths against two lake parameters. Past conditions (top), projected 2×CO₂ CCC GCM climate scenario (middle), and differences between 2×CO₂ and past climate conditions (bottom).

Table 3
Simulated characteristics of ice covers on Minnesota lakes under different climate scenarios

Maximum lake depth (m)	Climate scenario	Earliest dates of ice cover formation ^a	Latest dates of ice cover formation ^a	Earliest ice-out dates ^a	Latest ice-out dates ^a	Cumulative (total) days of ice cover	Total period of ice cover (days)
<i>Southern Minnesota lakes</i>							
4	Past	317 (6)	329 (7)	98 (9)	99 (8)	142 (8)	148 (10)
	GISS	336 (12)	349 (15)	63 (17)	67 (11)	88 (19)	102 (23)
	CCC	327 (11)	344 (15)	53 (20)	65 (15)	88 (19)	103 (24)
13	Past	328 (6)	331 (5)	99 (8)	99 (9)	137 (9)	137 (9)
	GISS	346 (9)	353 (12)	66 (17)	68 (13)	84 (19)	89 (23)
	CCC	337 (6)	346 (15)	56 (18)	59 (15)	83 (19)	89 (24)
24	Past	335 (5)	336 (5)	100 (9)	100 (9)	131 (9)	131 (9)
	GISS	352 (10)	359 (10)	66 (17)	67 (16)	77 (18)	81 (25)
	CCC	344 (7)	353 (20)	56 (18)	59 (15)	77 (21)	81 (25)
<i>Northern Minnesota lakes</i>							
4	Past	308 (8)	318 (8)	111 (6)	112 (6)	165 (8)	167 (9)
	GISS	324 (8)	337 (14)	84 (9)	85 (9)	118 (17)	127 (23)
	CCC	316 (6)	332 (13)	77 (15)	83 (11)	123 (15)	130 (25)
13	Past	318 (6)	321 (6)	112 (6)	112 (6)	160 (7)	162 (8)
	GISS	335 (5)	337 (6)	86 (9)	86 (9)	116 (11)	118 (17)
	CCC	328 (6)	335 (12)	81 (15)	82 (12)	117 (16)	119 (18)
24	Past	325 (5)	327 (6)	113 (6)	113 (6)	154 (7)	154 (7)
	GISS	341 (5)	341 (5)	86 (9)	86 (9)	111 (11)	112 (15)
	CCC	334 (6)	338 (9)	81 (15)	81 (14)	112 (17)	113 (18)

^a Julian dates. Numbers are for eutrophic lakes and are averages of three lake sizes ($A_S = 0.2, 1.7, \text{ and } 10 \text{ km}^2$). Numbers in parentheses are the standard deviation from the mean.

given winter. Discontinuous ice covers predominantly form at the beginning of winter. Therefore the latest ice-in date has also been extracted from the simulation results.

The *last (latest) ice-in date* in fall or winter is the date after which the ice cover exists continuously until spring ice-out. After this date no further aeration of the water surface occurs. This average date has been plotted as Julian day in Fig. 7a, and the standard deviation from this date based on 19 years of data is given in Fig. 7b. Standard deviation (STD) gives variation of this date in response to variation of weather input over 19 years. For reference, December 1 is Julian day 335. Trophic state has little effect on the ice-in date. Variations in lake morphometry cause variations of up to 6 days in the mean value of this date. Climate change is projected to delay this date by 2 to 3 weeks. Standard deviations from the mean date are now about 5 to 8 days and will increase to as much as 20 days in the south and 14 days in the north after climate change.

The *first ice-out date* is the first date in spring at which the ice cover has disappeared. Its average value has been plotted as Julian day in Fig. 8a, and the standard deviation from this average (in days) in Fig. 8b. Julian day 91 is April 1. Trophic state and geometry of a lake have little effect on ice-out date. Latitude is important. Ice-out presently occurs in northern Minnesota about 2 weeks after southern Minnesota (the difference is about 4 to 5 weeks from the southern to the northern border of Minnesota). After climate change the difference is projected to double from the present 2 weeks to 4 weeks. More importantly, ice-out dates will be about 6 to 7 weeks earlier in the south, and 4 to 5 weeks earlier in the north. This is a very substantial change, which is likely to eliminate fish winterkill (Stefan and Fang, 1995). Winterkill occurs mostly in shallow lakes when dissolved oxygen concentrations drop below 2 mg/l at all depths in early spring. Standard deviations from average dates of first ice-out are presently about 1 week and will increase to 2 weeks under $2 \times \text{CO}_2$ climate conditions.

Simulated ice cover characteristics are summarized in Table 3, which gives averages for three lake sizes ($A_s = 0.2, 1.7, 10 \text{ km}^2$). All parameters are independent of lake trophic state and only very weakly dependent on lake surface area. Table 3

emphasizes differences of ice cover characteristics with maximum lake depth. Standard deviations within parentheses indicate variations over the 19-year simulation period. The GISS and CCC climate projection models differ in their forecast (Fig. 3), and hence the effects on ice/snow covers also differ somewhat as shown in Table 3. Compared to the CCC model results, the GISS model input to the ice cover model delays ice formation and ice-out dates by about 1 week; therefore the period of ice cover is almost unchanged.

5. Summary and conclusions

An ice and snow cover model associated with a deterministic, one-dimensional water temperature model is presented for dimictic and polymictic lakes of the temperate zone. The lake parameters required as model input are surface area (A_s), maximum depth (H_{max}), and Secchi depth as a measure of light attenuation and trophic state. The model is driven by daily weather data and operates year-round over multiple years. The model has been validated with extensive data. Standard errors between simulated and measured values are 0.12 m for ice thicknesses on lakes, 0.07 m for snow covers, and less than 6 days for ice formation dates. The model has been applied to simulate effects of climate change on winter ice and snow covers of 27 lake types under Minnesota climate conditions. The projected climate changes due to a doubling of atmospheric CO_2 were obtained from the output of the Canadian Climate Center Global Circulation Model (CCC GCM) and the Goddard Institute of Space Studies at Columbia University (GISS GCM). To illustrate the effect of projected climate change on winter ice/snow cover characteristics, separate graphs are presented for values simulated with inputs of past climate conditions (1961–79) and with projected $2 \times \text{CO}_2$ climate scenarios.

Under the past climate (1961–79), the total *duration of ice cover* is about 140 days in the south, and about 160 days in the north. The periods will be shortened to about 85 days and 120 days under $2 \times \text{CO}_2$ climate scenarios, respectively. Variations in lake morphometry cause variations of up to 6 days in the mean value of the ice-in date. Trophic state

has little effect. Climate change is projected to delay this date by 2 to 3 weeks. The earliest *ice-out date* is the first date in spring at which the ice cover has disappeared. Trophic state and geometry of a lake have little effect on ice-out date, but latitude is important. Ice-out presently occurs in northern Minnesota about 2 weeks after southern Minnesota (the difference is about 4 to 5 weeks from the southern to the northern border of Minnesota). After climate change the difference is projected to double from the present 2 weeks to 4 weeks. More importantly, ice-out dates will be about 6 to 7 weeks earlier in the south, and 4 to 5 weeks earlier in the north. This is a very substantial change. Standard deviations from average dates are presently about 1 week and will increase to 2 weeks. Under a $2 \times \text{CO}_2$ climatic scenario, *maximum ice and snow thickness* are projected to be reduced by 50% or more. These changes during the winter would eliminate fish winterkill in most shallow lakes, but would endanger snowmobiles and fishermen because of the reduced bearing capacity of lake ice.

Acknowledgements

This study was supported by the U.S. Environmental Protection Agency, Mid-Continent Ecology Division, Duluth, MN and the Office of Research and Development, Washington, DC. John G. Eaton and Barbara M. Levinson were project officers. The Minnesota Supercomputer Institute, University of Minnesota, provided a resource grant and access to its CRAY-2 supercomputer.

References

- Ashton, G.D., 1986. River and Lake Ice Engineering. Water Resources Publications, Littleton, CO, 485 pp.
- Baker, D.G., Kuehnast, E.L. and Zandlo, J.A., 1985. Climate of Minnesota Part 15 — Normal Temperatures (1951-80) and Their Application. Agricultural Experimental Station, University of Minnesota, AD-SB-2777.
- Bannister, T.T., 1974. Prediction equations in terms of chlorophyll concentration, quantum yield, and upper limit of production. *Limnol. Oceanogr.*, 19(1): 1–12.
- Boer, G.J., McFarlane, N.A. and Lazare, M., 1992. Greenhouse gas-induced climate change simulated with the CCC second-generation general circulation model. *J. Clim.*, 5(10).
- Bolsenga, S.J., 1977. Preliminary observations of the daily variation of ice albedo. *J. Glaciol.*, 18: 517–521.
- Carslaw, H.S. and Jaeger, J.C., 1959. *Conduction of Heat in Solids*. Oxford University Press, New York, 510 pp.
- Dake, J.M.K. and Harleman, D.R.F., 1969. Thermal stratification in lakes: Analytical and laboratory studies. *Water Resour. Res.*, 5(2): 484–496.
- Edinger, J.E., Dutweiler, D.W. and Geyer, J.C., 1968. The response of water temperature to meteorological conditions. *Water Resour. Res.*, 4(5): 1137–1143.
- Ellis, C.E. and Stefan, H.G., 1997. Vertical thermal diffusivity in an ice-covered lake. *Water Resour. Bull.*, submitted.
- Fang, X. and Stefan, H.G., 1994. Temperature and dissolved oxygen simulations in a lake with ice cover. Project Report 356, St. Anthony Falls Hydraulic Laboratory, University of Minnesota, Minneapolis, MN.
- Fang, X. and Stefan, H.G., 1996a. Long-term lake water temperature and ice cover simulations/measurements. *Cold Reg. Sci. Technol.*, 24(3): 289–304.
- Fang, X. and Stefan, H.G., 1996b. Dynamics of sediment heat exchange in lakes. *Water Resour. Res.*, 32(6): 1719–1727.
- Fang, X., Ellis, C.E. and Stefan, H.G., 1996. Simulation and observation of ice formation (freeze-over) in a lake. *Cold Reg. Sci. Technol.*, 24: 129–145.
- Ford, D.E. and Stefan, H.G., 1980. Thermal predictions using integral energy model. *J. Hydraul. Div. ASCE*, 106(1): 39–55.
- Gorham, E. and Boyce, F.M., 1989. Influence of lake surface area and depth upon thermal stratification and the depth of the summer thermocline. *J. Great Lakes Res.*, 15: 233–245.
- Greene, G.M., 1981. Simulation of ice-cover growth and decay in one dimension on the upper St. Lawrence River. NOAA Technical Memorandum Erl GLERL-36.
- Gu, R. and Stefan, H.G., 1990. Year-round temperature simulation of cold climate lakes. *Cold Reg. Sci. Technol.*, 18(2): 147–160.
- Harleman, D.R.F., 1982. Hydrothermal analysis of lakes and reservoirs. *J. Hydraul. Div. ASCE*, 108(HY3): 39–49.
- Heiskary, S.A., Wilson, C.B. and Larsen, D.P., 1987. Analysis of regional patterns in lake water quality: Using ecoregions for lake management in Minnesota. *Lake Reservoir Management*, 3: 337–344.
- Hondzo, M. and Stefan, H.G., 1993a. Lake water temperature simulation model. *J. Hydraul. Eng. ASCE*, 119(11): 1251–1273.
- Hondzo, M. and Stefan, H.G., 1993b. Regional water temperature characteristics of lakes subjected to climate change. *Clim. Change*, 24: 187–211.
- Lock, G.S.H., 1934. *The Growth and Decay of Ice*. Cambridge University Press, 434 pp.
- McFarlane, N.A., Boer, G.J., Blanchet, J.P. and Lazare, M., 1992. The Canadian Climate Center second-generation general circulation model and its equilibrium climate. *J. Clim.*, 5(10).
- Megard, R.O., Combs, W.S., Simth, P.D. and Knoll, A.S., 1979. Attenuation of light and daily integral rates of photosynthesis attained by planktonic algae. *Limnol. Oceanogr.*, 24(6): 1038–1050.
- Pivovarov, A.A., 1972. *Thermal Condition in Freezing Lakes and Rivers*. Wiley, New York, NY.

- Riley, M.J. and Stefan, H.G., 1987. A dynamic lake water quality simulation model. *Ecol. Modelling*, 43: 155–182.
- Scott, J.T., 1964. A comparison of the heat balance of lakes in winter. Technical Report 13, University of Wisconsin, Department of Meteorology, Madison, WI.
- Stefan, H.G. and Fang, X., 1995. A methodology to estimate year-round effects of climate change on water temperature, ice and dissolved oxygen characteristics of temperate zone lakes with application to Minnesota. Project Report No. 377, St Anthony Falls Hydraulic Laboratory, University of Minnesota, Minneapolis, MN.
- Stefan, H.G., Hondzo, M., Sinokrot, B., Fang, X., Eaton, J.G., Goodno, B.E., Hokanson, K.E.F., McCormick, J.H., O'Brien, D.G. and Wisniewski, J.A., 1992. A methodology to estimate global climate change impacts on lake and stream environmental conditions and fishery resources with application to Minnesota. Project Report No. 323, St Anthony Falls Hydraulic Laboratory, University of Minnesota, Minneapolis, 141 pp.
- Stefan, H.G., Hondzo, M. and Fang, X., 1993. Lake water quality modeling for projected $2\times\text{CO}_2$ climate scenarios. *J. Environ. Qual.*, 22(3): 417–431.
- Wake, A. and Rumer, R.R., 1979. Modeling the ice regime of Lake Erie. *J. Hydraul. Eng. ASCE*, 105: 827–844.